Spectral functions, Fermi surface, and pseudogap in the t-J model

P. Prelovšek and A. Ramšak
Faculty of Mathematics and Physics, University of Ljubljana, 1111 Ljubljana, Slovenia
and J. Stefan Institute, University of Ljubljana, 1111 Ljubljana, Slovenia
(Received 3 September 2001; revised manuscript received 26 November 2001; published 7 May 2002)

Spectral functions within the generalized t-J model as relevant to cuprates are analyzed using the method of equations of motion for projected fermion operators. In the evaluation of the self-energy a decoupling of spin and single-particle fluctuations is performed. It is shown that in an undoped antiferromagnet the method reproduces the self-consistent Born approximation. For finite doping with short-range antiferromagnetic order the approximation evolves into a paramagnon contribution which retains a large incoherent contribution in the hole part of the spectral function as well as the hole-pocket-like Fermi surface at low doping. On the other hand, the contribution of longer-range spin fluctuations, with the coupling mostly determined predominantly by J and next-neighbor hopping t', is essential for the emergence of the pseudogap. The latter shows, at low doping in the effective truncation of the large Fermi surface, a reduced electron density of states and at the same time a quasiparticle density of states at the Fermi level.

DOI: 10.1103/PhysRevB.65.174529 PACS number(s): 71.27.+a, 72.15.−v, 71.10.Fd

I. INTRODUCTION

One of the central issues in the experimental and theoretical investigations of superconducting cuprates is the understanding of low-energy electronic excitations in these compounds.[1] In recent years, angle-resolved photoemission spectroscopy (ARPES) experiments revealed quite a universal development of electron spectral properties as a function of doping. In most investigated $Bi_2Sr_2CaCu_2O_{2+\delta}$ (BSCCO) ARPES shows quite well-defined large Fermi surface in the overdoped and optimally doped samples at $T>T_c$, whereby the low-energy behavior with increasing doping in the overdoped regime qualitatively approaches (but does not in fact reach) that of a normal Fermi liquid with underdamped quasiparticle (QP) excitations. On the other hand, in underdoped materials the QP's dispersing through the Fermi surface (FS) are resolved by ARPES in BSCCO only in parts of the large FS, in particular along the nodal $(0,0)$-(π,π) direction,[2] indicating that the rest of the large FS is truncated,[3] i.e., either fully or effectively gapped. At the same time near the $(\pi,0)$ momentum ARPES reveals a hump at ~ 100 meV,[2] which indicates the existence of a pseudogap scale, which is consistent with the characteristic temperature pseudogap scale $T^*>T_c$, which appears also as a crossover in several other quantities: the uniform susceptibility $\chi(T)$, resistivity $\rho(T)$, specific heat $C_V(T)$, and Hall constant $R_H(T)$.[1] Although the latter anomalies in thermodynamic and transport quantities are also quite similar (or even better confirmed and more pronounced) in $La_{2-x}Sr_xCu_2O_4$ (LSCO), spectral properties of the latter[4] are qualitatively different from those of BSCCO, presumably due to the crucial role of stripe structures in LSCO in the regime of intermediate doping.

There appears to be quite a consensus on the spectral functions in an undoped two-dimensional (2D) reference antiferromagnet (AFM), describing a single hole behaving as a QP with a strongly renormalized mass and a large incoherent component. The spectral function is well captured within the self-consistent Born approximation[5,6] (SCBA) for the simplest relevant t-J model, whereby for an agreement with underdoped cuprates[7,8] longer-range hopping terms have been invoked.[9,10]

For larger (finite) doping, numerical approaches have been used extensively, employing mainly the exact-diagonalization and quantum Monte Carlo methods for prototype models such as the Hubbard model and the t-J model. Results confirm some gross features consistent with experiments, in particular: (a) the existence of a large FS in a moderately doped AFM (Refs. 11 and 9); (b) the overdamped character of a QP at intermediate doping,[12,13] consistent with the marginal Fermi-liquid concept;[14] (c) pseudogap features at lower doping in spectral functions[15] and in the density of states (DOS) (Ref. 13); and (d) a quite visible contribution of longer-range hopping.[10] However, numerical studies in general are not in a position to approach effectively the low-energy regime, and results require a proper phenomenological interpretation.

Analytical approximations of spectral properties in 2D strongly correlated systems at finite doping have proven to be very delicate. For the one-band Hubbard model spectral functions have been evaluated within the random-phase approximation[16] and within the self-consistent conserving theory,[17] both restricted to moderate U/t. Strong correlations are explicitly taken into account in slave boson theories.[18] Antiferromagnetic spin fluctuations play an essential role in phenomenological theory of the spin-fermion model,[19] where recently aspects of the pseudogap features in the underdoped regime have also been found.[20,21]

Concerning the origin of the pseudogap scale, it seems to be related to the exchange J since $T^*\sim J$ in low doping materials, whereas $T^*\sim T_c$ in optimally doped samples. Evidence that antiferromagnetic spin correlations are important for the (large) pseudogap also comes from the numerical studies[15,12,13] and phenomenological model studies.[20,21] Renormalization-group studies of the Hubbard model[22] (with moderate U/t) also revealed the instability of a normal Fermi liquid close to the half-filled band (insulator), and a possible truncation of the Fermi surface.

One of present authors introduced the equations-of-

motion (EQM) method[23] for the evaluation of the spectral functions within the t-J model. It has been shown that EQM for projected fermionic operators implicitly reveal an effective spin-fermion coupling. It was possible to relate the overdamped marginal-type character of a QP to the marginal dynamics of spins[23] and to treat the onset of d-wave superconductivity.[24] Recently the EQM method has also been applied to the Hubbard model.[25] Within the t-J model the theory has been improved[26] by a more appropriate treatment of the self-energy by dealing separately with (a) the strong coupling to short-range AFM spin fluctuations (paramagnons), and (b) the moderate coupling to longer-range fluctuations of the AFM order parameter. The aim of this paper is to present the results of the theory in more detail, in particular the evolution of spectral function as a function of doping. The emphasis is on the results at $T=0$ for (a) the development of the FS from a hole pocket like into a large one, (b) the emergence of the pseudogap in spectral functions and related effective truncation of the FS, (c) anomalous properties of QP at the FS, and (d) the depleted DOS and QP DOS (related to the specific-heat coefficient) with doping.

The paper is organized as follows: In Sec. II the EQM method for the spectral function within the t-J model is summarized. Section III is devoted to the evaluation of the self-energy within the decoupling approximation separately treating the paramagnon contribution $\Sigma_{\rm pm}$ and the contribution of longitudinal spin fluctuations $\Sigma_{\rm lf}$. In Sec. IV results of the simplified analysis of the pseudogap features are presented, taking into account an effective renormalized band and explicitly $\Sigma_{\rm lf}$. Section V presents results of the full self-consistent solution for spectral function as a function of doping.

II. EQUATIONS OF MOTION

In order to take strong correlations explicitly into account we study the t-J model

$$H=-\sum_{i,j,s} t_{ij}\tilde{c}^{\dagger}_{js}\tilde{c}_{is}+J\sum_{\langle ij\rangle}\left(\mathbf{S}_i\cdot\mathbf{S}_j-\frac{1}{4}n_in_j\right), \tag{1}$$

where fermionic operators are projected ones not allowing for the double occupancy of sites, i.e.,

$$\tilde{c}^{\dagger}_{is}=(1-n_{i,-s})c^{\dagger}_{is}. \tag{2}$$

Since longer-range hopping appears to be important for a proper description of the spectral function in cuprates, both for the shape of the FS at optimum doping materials[10] as well as for the explanation of ARPES of undoped insulators,[7,8,10] we consider, besides $t_{ij}=t$ for the nearest-neighbor hopping, $t_{ij}=t'$ for the next-nearest-neighbor hopping on a square lattice.

Our goal is to evaluate the electron Green's function (propagator) directly for projected fermionic operators,

$$G(\mathbf{k},\omega)=\langle\langle\tilde{c}_{\mathbf{k}s};\tilde{c}^{\dagger}_{\mathbf{k}s}\rangle\rangle_{\omega}=-i\int_0^{\infty}e^{i(\omega+\mu)t}\langle\{\tilde{c}_{\mathbf{k}s}(t),\tilde{c}^{\dagger}_{\mathbf{k}s}\}_+\rangle dt, \tag{3}$$

which is equivalent to the usual propagator within the allowed basis states of the model [Eq. (1)]. In the EQM method[27] one uses relations for general correlation functions

$$\begin{aligned}\omega\langle\langle A;B\rangle\rangle_{\omega}&=\langle\{A,B\}_+\rangle+\langle\langle[A,H];B\rangle\rangle_{\omega}\\&=\langle\{A,B\}_+\rangle-\langle\langle A;[B,H]\rangle\rangle_{\omega}.\end{aligned} \tag{4}$$

and applies the propagator $G(\omega)=\langle\langle A;A^{\dagger}\rangle\rangle_{\omega}$. If we define the (orthogonal) operator C as

$$[A,H]=\zeta A-iC,\quad \langle\{C,A^{\dagger}\}_+\rangle=0, \tag{5}$$

we can express

$$G(\omega)=G_0(\omega)+\frac{1}{\alpha^2}G_0(\omega)^2\langle\langle C;C^{\dagger}\rangle\rangle_{\omega},$$

$$G_0(\omega)=\frac{\alpha}{\omega-\zeta},\quad \alpha=\langle\{A,A^{\dagger}\}_+\rangle. \tag{6}$$

Identifying the self-energy $\Sigma(\omega)$ as the irreducible part of $\langle\langle C;C^{\dagger}\rangle\rangle_{\omega}$ we can express Eq. (6) as

$$G(\omega)=\frac{\alpha}{\omega-\zeta-\Sigma(\omega)},\quad \Sigma(\omega)\sim\frac{1}{\alpha}\langle\langle C;C^{\dagger}\rangle\rangle^{irr}_{\omega}. \tag{7}$$

Within the diagrammatic technique $\Sigma(\omega)$ corresponds to the contribution of irreducible diagrams. Generally $\Sigma(\omega)$ can be defined as a memory function within the Mori projection method.[28] In most cases the successful application of the method relies on the appropriate decoupling or other approximation of the memory function $\Sigma(\omega)$.[29]

Applying the formalism to the propagator [Eq. (3)], we have to deal with the EQM for $\tilde{c}^{\dagger}_{\mathbf{k}s}$ with a nontrivial normalization factor:

$$\alpha=\frac{1}{N}\sum_i\langle\{\tilde{c}_{is},\tilde{c}^{\dagger}_{is}\}_+\rangle=1-\frac{c_e}{2}=\frac{1}{2}(1+c_h). \tag{8}$$

By taking the projection in Eq. (2), explicitly into account the EQM follow,

$$\begin{aligned}[\tilde{c}_{is},H]=&-\sum_j t_{ij}[(1-n_{i,-s})\tilde{c}_{js}+S^{\mp}_i\tilde{c}_{j,-s}]\\&+\frac{1}{4}J\sum_{jn.n.i}(2sS^z_j\tilde{c}_{is}+2S^{\mp}_j\tilde{c}_{i,-s}-n_j\tilde{c}_{is})\end{aligned} \tag{9}$$

with $s=\pm1$. We express "bosonic" variables in terms of spin and density operators, i.e., $n_{i,-s}=n_i/2-sS^z_i$. Assuming that we are dealing with a paramagnetic metal with $\langle\mathbf{S}_i\rangle=0$ and a homogeneous electron density $\langle n_i\rangle=c_e$, we obtain

$$-iC_{\mathbf{k}s}=[\tilde{c}_{\mathbf{k}s},H]-\zeta_{\mathbf{k}}\tilde{c}_{\mathbf{k}s}, \tag{10}$$

and

$$[\tilde{c}_{\mathbf{k}s},H]=\left[\left(1-\frac{c_e}{2}\right)\epsilon^0_{\mathbf{k}}-Jc_e\right]\tilde{c}_{\mathbf{k}s}+\frac{1}{\sqrt{N}}\sum_{\mathbf{q}} m_{\mathbf{kq}}\Big[sS^z_{\mathbf{q}}\tilde{c}_{\mathbf{k}-\mathbf{q},s} + S^{\mp}_{\mathbf{q}}\tilde{c}_{\mathbf{k}-\mathbf{q},-s}-\frac{1}{2}\tilde{n}_{\mathbf{q}}\tilde{c}_{\mathbf{k}-\mathbf{q},s}\Big], \tag{11}$$

where $\tilde{n}_i=n_i-c_e$, $m_{\mathbf{kq}}$ is the effective spin-fermion coupling,

$$m_{\mathbf{kq}}=2J\gamma_{\mathbf{q}}+\epsilon^0_{\mathbf{k}-\mathbf{q}} \tag{12}$$

with the bare band dispersion $\epsilon^0_{\mathbf{k}}$, i.e., for model (1) on a square lattice,

$$\epsilon^0_{\mathbf{k}}=-4t\gamma_{\mathbf{k}}-4t'\gamma'_{\mathbf{k}}, \tag{13}$$

$$\gamma_{\mathbf{k}}=\tfrac{1}{2}(\cos k_x+\cos k_y),\quad \gamma'_{\mathbf{k}}=\cos k_x\cos k_y .$$

Equations (4), (11), and (13) also define the ''renormalized'' band

$$\zeta_{\mathbf{k}}=\frac{1}{\alpha}\langle\{[\tilde{c}_{\mathbf{k}s},H],\tilde{c}^{\dagger}_{\mathbf{k}s}\}_+\rangle=\overline{\zeta}-4\eta_1 t\gamma_{\mathbf{k}}-4\eta_2 t'\gamma'_{\mathbf{k}},$$

$$\eta_j=\alpha+\frac{1}{\alpha}\langle\mathbf{S}_0\cdot\mathbf{S}_j\rangle, \tag{14}$$

where η_j are determined solely by short-range spin correlations and $\overline{\zeta}$ is a $\mathbf{k}$-independent term (still dependent on various static correlations). The above quantities determine the propagator

$$G(\mathbf{k},\omega)=\frac{\alpha}{\omega+\mu-\zeta_{\mathbf{k}}-\Sigma(\mathbf{k},\omega)}, \tag{15}$$

and the corresponding spectral function $A(\mathbf{k},\omega)=-(1/\pi)\mathrm{Im}\,G(\mathbf{k},\omega)$, provided that we find a method to evaluate $\Sigma(\mathbf{k},\omega)$.

III. SELF-ENERGY

A. Undoped antiferromagnet

It is desirable that in the case of an undoped AFM our treatment of Σ and the spectral function reproduces quite successful SCBA equations[5,6] for the Green's function of a hole in an AFM. Let us concentrate here on the relevant nearest-neighbor hopping, since the t' term represents a hopping on the same sublattice within an ordered AFM and is therefore nearly free. For the SCBA the reference state is the Néel state with $n_{is}=0,1$ for $i=A,B$ sublattices, respectively, and the SCBA effective Hamiltonian can be written as

$$H_h=-t\sum_{\langle ij\rangle}(h_i h^{\dagger}_j a_j+h_j h^{\dagger}_i a^{\dagger}_j)+H_J, \tag{16}$$

where h_i represent holon operators and a_i spin-flip operators. The corresponding holon EQM then follow from Eq. (16):

$$-i\frac{d}{dt}h^{\dagger}_i=[h_i,H_h]=t\sum_{jn.n.i} h^{\dagger}_j(a^{\dagger}_i+a_j). \tag{17}$$

It is now straightforward to establish the relation of Eq. (17) with the EQM for $\tilde{c}_{is}$ by considering one Néel sublattice $i=A$ with the reference state $n_{is}=1$. In this case $1-n_{i,-s}=1$, and by a formal replacement $\tilde{c}_{js}=\tilde{c}_{j,-s}S^{\mp}_j$ we obtain, by considering only the t term in Eq. (9),

$$i\frac{d}{dt}\tilde{c}_{is}\sim -t\sum_{n.n.i}(S^{\mp}_i+S^{\mp}_j)\tilde{c}_{j,-s}. \tag{18}$$

To be consistent with the SCBA here we neglect the J term in Eq. (9) since $J\ll t$. Within the linearized magnon theory EQM (17) and (18) are formally identical, so we can further follow the procedure of the evaluation of $\Sigma_{\mathrm{AFM}}(\mathbf{k},\omega)$ within the SCBA to reproduce spectral properties of an undoped AFM. In this case we do not try to improve the SCBA, since the latter approximation is simple and yields both qualitatively and quantitatively good results consistent with numerical studies and experiments. Vertex corrections are neglected in the SCBA, but are expected to be of small relevance, due to vanishing of the lowest order crossing diagrams, as discussed in Refs. 6. For an ordered 2D AFM where relevant spin excitations are magnons with dispersion $\omega_{\mathbf{q}}$, we therefore obtain

$$\Sigma_{\mathrm{AFM}}(\mathbf{k},\omega)=\frac{1}{N}\sum_{\mathbf{q}} M^2_{\mathbf{kq}}G(\mathbf{k}-\mathbf{q},\omega+\omega_{\mathbf{q}}),$$

$$M_{\mathbf{kq}}=4t(u_{\mathbf{q}}\gamma_{\mathbf{k}-\mathbf{q}}+v_{\mathbf{q}}\gamma_{\mathbf{k}}), \tag{19}$$

with

$$u_{\mathbf{q}}=\sqrt{\frac{2J+\omega_{\mathbf{q}}}{2\omega_{\mathbf{q}}}},\quad v_{\mathbf{q}}=-\mathrm{sgn}(\gamma_{\mathbf{q}})\sqrt{\frac{2J-\omega_{\mathbf{q}}}{2\omega_{\mathbf{q}}}},$$

$$\omega_{\mathbf{q}}=2J\sqrt{1-\gamma^2_{\mathbf{q}}}. \tag{20}$$

Since in a Néel state we have $\eta_1=0$ and hence the renormalized band vanishes, i.e., $\zeta_{\mathbf{k}}=0$, we reproduce the usual SCBA equations for the hole spectral function in the t-J model. The inclusion of the next-nearest-neighbor hopping t' is also simple within the SCBA, since within the Néel state it does not induce a coupling to spin flips in Eq. (9) and therefore enters into $G(\mathbf{k},\omega)$ [Eq. (15)], only via the band term $\zeta_{\mathbf{k}}\sim\overline{\zeta}-4t'\gamma'_{\mathbf{k}}$. It should also be noted that in contrast to the usual SCBA our procedure deals directly with the electron propagator and not with an unphysical holon one. Moreover it allows a straightforward generalization to the case of finite doping.

B. Short-range spin fluctuations

For finite doping $c_h>0$ we assume that spin fluctuations remain dominant at the antiferromagnetic wave vector $\mathbf{Q}=(\pi,\pi)$ with the characteristic inverse antiferromagnetic correlation length $\kappa=1/\xi_{AFM}$. The latter seems to be the case for BSCCO as well as $YB_2Cu_3O_{6+x}$, but not for LSCO with pronounced stripe and spin-density structures with

$\mathbf{q}_{SDW} \neq \mathbf{Q}$. For the former case one can divide the spin fluctuations and their coupling to fermions into two regimes with respect to $\tilde{\mathbf{q}} = \mathbf{q} - \mathbf{Q}$.

(a) At short distances, i.e., for $\tilde{q} > \kappa$, the short-range correlations between the fermion and background spin are important. As in an ordered AFM in Eq. (18), the fermion couples only to short-range spin fluctuations paramagnons, which are propagating like magnons and are transverse to the local antiferromagnetic short-range spin ordering. Hence it makes sense to use Eqs. (19) and (20) to represent the paramagnon contribution to the self-energy, restricting the sum to the regime $\tilde{q} > \kappa$.

(b) For $\tilde{q} < \kappa$ spin fluctuations are essentially not propagating modes but rather critically overdamped. Fluctuations recover full spin rotation symmetry so deviations from the ordered AFM state are essential. A more appropriate approximation of $\Sigma(\mathbf{k}, \omega)$ is to take the fermion and background spin fluctuations as independent, as discussed in Sec. III C.

We should also take into account that the SCBA formalism has been derived for an undoped AFM, i.e., for a hole spectral function at $\omega < 0$, where only (added) holes participate. Since we are dealing with $c_h > 0$, we take into account the scattering of a holelike ($\omega < 0$) QP by replacing the full propagator G in Eq. (19) by the hole part G^-:

$$G^{\mp}(\mathbf{k}, \omega) = \pm \int_{\mp\infty}^{0} \frac{d\omega' A(\mathbf{k}, \omega')}{\omega - \omega'}, \tag{21}$$

However it is easy to see that an analogous contribution should arise from the electronlike QP with $\omega > 0$. At the finite doping case we therefore generalize (at $T = 0$) Eq. (19) into the paramagnon contribution

$$\Sigma_{\rm pm}(\mathbf{k}, \omega) = \frac{1}{N} \sum_{q, \tilde{q} > \kappa} [M^2_{\mathbf{kq}} G^-(\mathbf{k} - \mathbf{q}, \omega + \omega_{\mathbf{q}}) + M^2_{\mathbf{k}+\mathbf{q},\mathbf{q}} G^+(\mathbf{k} + \mathbf{q}, \omega - \omega_{\mathbf{q}})], \tag{22}$$

which emerges from Eq. (18). The consequence of Eq. (22) is that in general $\mathrm{Im}\,\Sigma_{\rm pm}(\mathbf{k}, \omega > 0) \neq 0$ so that an electronlike QP can also be damped due to magnon processes. Here we do not consider effects of $T > 0$ which could be easily incorporated through the magnon occupation, but in most cases do not have a strong influence at low $T < J$.

Here we stress two features of our approximation for paramagnon contribution $\Sigma_{\rm pm}$:

(a) we are dealing with a strong coupling theory due to $t > \omega_{\mathbf{q}}$ and a self-consistent calculation of $\Sigma_{\rm pm}$ is required; and (b) the resulting $\Sigma_{\rm pm}(\mathbf{k}, \omega)$ as well $A(\mathbf{k}, \omega)$ are at low doping quite asymmetric with respect to $\omega = 0$. Here as in an undoped AFM the hole part G^- with the weight, $\propto (1 - c_h)/2 \sim 1/2$, generates a large incoherent part in $A(\mathbf{k}, \omega \ll 0)$. On the other hand, G^+ has less weight $\propto c_h$, and consequently the scattering of an electron QP is in general much less effective.

C. Coupling to longer-range spin fluctuations

Discussing the self-energy at finite doping, Eq. (22) represents only one contribution and we have to reconsider EQM (10) and (11). We note that at $c_h > 0$ $C_{\mathbf{ks}}$ contains a remainder of a ''free'' term $\propto \tilde{c}_{\mathbf{ks}}$, which should be, however, neglected when evaluating the ''irreducible'' part entering Σ [Eq. (7)]. Considering within the simplest approximation only the mode-coupling terms in Eq. (11), we also neglect the coupling to density fluctuation $\tilde{n}_{\mathbf{q}}$ which should contribute much less to Σ in the absence of charge ordering or charge instabilities at low doping.

Taking into account only spin fluctuations, at $c_h > 0$ we are dealing with a paramagnet without an antiferromagnetic long-range order, and besides the paramagnon excitation with $\tilde{q} > \kappa$ the coupling to longer-range spin fluctuations with $\tilde{q} < \kappa$ also becomes crucial. The latter restore the spin rotation symmetry in a paramagnet and equation of motion (11) naturally introduces such a spin-symmetric coupling. Assuming within a simplest approximation that the dynamics of fermions and spins is independent,

$$\langle S^z_{\mathbf{q}}(t) \tilde{c}_{\mathbf{k}-\mathbf{q},s}(t) S^z_{-\mathbf{q}'} \tilde{c}^{\dagger}_{\mathbf{k}-\mathbf{q}',s} \rangle \sim \delta_{\mathbf{qq}'} \langle S^z_{\mathbf{q}}(t) S^z_{-\mathbf{q}} \rangle \langle \tilde{c}_{\mathbf{k}-\mathbf{q},s}(t) \tilde{c}^{\dagger}_{\mathbf{k}-\mathbf{q},s} \rangle, \tag{23}$$

for contributions from longer-range (for convenience termed longitudinal) fluctuations we obtain

$$\Sigma_{\rm lf}(\mathbf{k}, \omega) = \frac{r_s}{\alpha} \sum_{\mathbf{q}} \tilde{m}^2_{\mathbf{kq}} \int \int \frac{d\omega_1 d\omega_2}{\pi} g(\omega_1, \omega_2) \times \frac{\tilde{A}(\mathbf{k} - \mathbf{q}, \omega_1) \chi''(\mathbf{q}, \omega_2)}{\omega - \omega_1 - \omega_2},$$

$$g(\omega_1, \omega_2) = f(-\omega_1) + \overline{n}(\omega_2) = \frac{1}{2} \left[\tanh \frac{\beta \omega_1}{2} + \coth \frac{\beta \omega_2}{2} \right], \tag{24}$$

where χ is the dynamical spin susceptibility:

$$\chi(\mathbf{q}, \omega) = -i \int_0^{\infty} e^{i\omega t} \langle [S^z_{\mathbf{q}}(t), S^z_{-\mathbf{q}}] \rangle dt. \tag{25}$$

Such an approximation for Σ has been introduced within the t-J model in Ref. 23. However, quite an analogous treatment has been employed previously in the Hubbard model[16] and more recently within the spin-fermion model.[20,21] Several comments are in order to define quantities entering Eq. (25):

(a) Equation of motion (11) induces an effective spin-fermion coupling, which would also emerge from a phenomenological spin-fermion Hamiltonian with the coupling parameter $m_{\mathbf{kq}}$ [Eq. (12)]. In order that such a Hamiltonian is hermitian, the coupling should satisfy

$$\tilde{m}_{\mathbf{k},\mathbf{q}} = \tilde{m}_{\mathbf{k}-\mathbf{q},-\mathbf{q}}, \tag{26}$$

which is in general not the case with the form Eq. (12); therefore we use, further on, instead the symmetrized coupling

$$\tilde{m}_{\mathbf{kq}} = 2J\gamma_{\mathbf{q}} + \frac{1}{2}(\epsilon^0_{\mathbf{k}-\mathbf{q}} + \epsilon^0_{\mathbf{k}}). \tag{27}$$

Here we should point out that in contrast to previous related studies of phenomenological spin-fermion coupling,[16,20,21] our $\tilde{m}_{\mathbf{kq}}$ (as well as $m_{\mathbf{kq}}$) is strongly dependent on both $\mathbf{q}$ and $\mathbf{k}$. It is essential that in the most sensitive parts of the FS, i.e., along the antiferromagnetic zone boundary (''hot'' spots, where $k=|\mathbf{Q}-\mathbf{k}|$), the coupling is in fact quite moderate and determined solely by J and t'.

(b) Since we are dealing with the paramagnetic state, all quantities should be spin invariant, i.e., $\chi^{\alpha\beta}(\mathbf{q},\omega) = \delta_{\alpha\beta}\chi(\mathbf{q},\omega)$. Since equaiton of motion (11) is invariant under spin rotations we have, besides the S^z term, analogous terms with S^- and S^+. Still we expect $r_s=1$ instead of $r_s=3$, since predominantly the coupling to longitudinal (to local Néel spin order) spin fluctuations is considered here, while the coupling to short-range transverse fluctuations has been already taken into account by $\Sigma_{\rm pm}$.

(c) In $\Sigma_{\rm lf}$ only the part corresponding to irreducible diagrams should enter, so there are restrictions on the proper decoupling. We will be interested mostly in the situation with a pronounced antiferromagnetic short-range order where longitudinal fluctuations are slow, i.e., with the characteristic frequencies $\omega_\kappa \lesssim 2J\kappa \ll J$. The regime is close to that of quasistatic $\chi(\mathbf{q},\omega)$ where the simplest and also quite satisfactory approximation is to insert for $\tilde{A}$ the unrenormalized A^0, the latter corresponding in our case to the spectral function without $\Sigma_{\rm lf}$ but with $\Sigma=\Sigma_{\rm pm}$. Such an approximation has been introduced in the theory of a pseudogap in charge-density-wave systems,[30] also used in related works analyzing the role spin fluctuations,[16,20] and recently more extensively examined in Ref. 31. In the opposite case of a full self-consistent treatment with $\tilde{A}=A$, we would overcount the influence of fluctuations, although the results would probably appear not so much different as shown on simpler systems.[31]

For $\chi(\mathbf{q},\omega)$ [Eq. (25)], at $c_h>0$ and possibly $T>0$, we do not have a corresponding theory, so we treat it as an input, where $\chi(\mathbf{q},\omega)$ is restricted by the sum rule

$$\frac{1}{N}\sum_{\mathbf{q}} \int_0^\infty \coth\left(\frac{\beta\omega}{2}\right)\chi''(\mathbf{q},\omega)d\omega = \frac{\pi}{4}(1-c_h). \tag{28}$$

At the same time, the system is close to the antiferromagnetic instability, so we assume spin fluctuations of the overdamped form[19]

$$\chi''(\mathbf{q},\omega) \propto \frac{\omega}{(\tilde{q}^2+\kappa^2)(\omega^2+\omega_\kappa^2)}. \tag{29}$$

For convenience we choose the separable form, which is consistent with experimental facts and theoretical arguments for $\tilde{q}<\kappa$ and $\omega<\omega_\kappa$. Nevertheless, at given κ and ω_κ the appearance of the pseudogap and the form of the FS is not very sensitive to the particular form of $\chi''(\mathbf{q},\omega)$ provided that $\chi''(\mathbf{q},\omega)$ is not singular as, e.g., is the case in the marginal Fermi-liquid scenario.[14] It has been shown[23] that the latter form is needed to obtain a generally overdamped QP with a vanishing QP weight (at $T=0$) in spectral functions at the intermediate doping.

IV. PSEUDOGAP ANALYSIS

Full calculation of the spectral functions $A(\mathbf{k},\omega)$ within the presented theory requires a self-consistent solution for $\Sigma=\Sigma_{\rm pm}+\Sigma_{\rm lf}$, where, besides the model parameters t, t', J and the doping c_h, inputs are μ,κ,η_1,η_2. κ, η_1, and η_2 are also given by short-range spin correlations dependent mostly on c_h, and can be taken from various analytical[32] and numerical[33,9] calculations within the t-J model. At the same time in a selfconsistent theory μ should be fixed via the DOS

$$\mathcal{N}(\omega) = \frac{2}{N}\sum_{\mathbf{k}} A(\mathbf{k},\omega), \tag{30}$$

with

$$c_h = 1 - \int_{-\infty}^{\infty} f(\omega)\mathcal{N}(\omega)d\omega. \tag{31}$$

Results of such a self-consistent calculation are presented in Sec. V.

In order to establish characteristic features of the pseudogap and the development of the FS we first perform a simplified analysis. We note that the effects of $\Sigma_{\rm pm}$ are threefold.

(a) $\Sigma_{\rm pm}$ induces a large incoherent component in the spectral functions at $\omega \ll 0$, in particular at low and intermediate dopings.

(b) $\Sigma_{\rm pm}$ renormalizes the effective QP band relevant to the behavior at $\omega\sim 0$ and at the FS.

(c) $\Sigma_{\rm pm}$ causes a transition of a large FS into a small hole-pocket-like FS at $c_h<c_h^*\ll 1$,

Result (b) can serve as a starting point for the discussion of the pseudogap and FS features at finite doping. If we define the effective band as

$$\epsilon^{\rm ef}_{\mathbf{k}} = Z^{\rm ef}_{\mathbf{k}}[\zeta_{\mathbf{k}} + \Sigma_{\rm pm}(\mathbf{k},0) - \mu],$$
$$Z^{\rm ef}_{\mathbf{k}} = \left[1 - \frac{\partial\Sigma_{\rm pm}(\mathbf{k},\omega)}{\partial\omega}\bigg|_{\omega=0}\right]^{-1}, \tag{32}$$

for the effective spectral function we obtain

$$A^0_{\rm ef}(\mathbf{k},\omega) = \alpha Z^{\rm ef}_{\mathbf{k}}\delta(\omega+\mu-\epsilon^{\rm ef}_{\mathbf{k}}), \tag{33}$$

which can be used to evaluate $\Sigma_{\rm lf}$. We restrict ourselves here to the regime of intermediate (not too small) doping, where $\epsilon^{\rm ef}_{\mathbf{k}}$ defines the large FS.

Let us concentrate on results for $T=0$. The simplest situation where $\Sigma_{\rm lf}$ can be evaluated analytically is the quasistatic and single-mode approximation (QSA) which is meaningful if $\omega_\kappa \ll t,\kappa \ll 1$. In this case we insert into Eq. (25)

$$\frac{1}{\pi}\chi''(\mathbf{q},\omega) \sim \frac{1}{4}\delta(\mathbf{q}-\mathbf{Q})[\delta(\omega-\nu)-\delta(\omega+\nu)], \tag{34}$$

with $\nu\to 0$. We obtain

$$\Sigma_{\rm lf}^{QSA}(\mathbf{k},\omega)=\frac{r_s m_{\mathbf{kQ}}^2}{4}\frac{Z^{\rm ef}_{\mathbf{k}-\mathbf{Q}}}{\omega-\epsilon^{\rm ef}_{\mathbf{k}-\mathbf{Q}}} \tag{35}$$

and

$$G^{QSA}(\mathbf{k},\omega)=\frac{\alpha Z^{\rm ef}_{\mathbf{k}}(\omega-\epsilon^{ef}_{\mathbf{k}-\mathbf{Q}})}{(\omega-\epsilon^{\rm ef}_{\mathbf{k}-\mathbf{Q}})(\omega-\epsilon^{\rm ef}_{\mathbf{k}})-\Delta^2_{\mathbf{k}}}, \tag{36}$$

$$\Delta^2_{\mathbf{k}}=\frac{r_s}{4}Z^{\rm ef}_{\mathbf{k}}Z^{\rm ef}_{\mathbf{k}-\mathbf{Q}}m^2_{\mathbf{kQ}}.$$

The spectral functions show in this approximation two branches of $E^{\pm}$, separated by the gap which opens along the antiferromagnetic zone boundary $\mathbf{k}=\mathbf{k}_{AFM}$, where $\epsilon^{\rm ef}_{\mathbf{k}-\mathbf{Q}}=\epsilon^{\rm ef}_{\mathbf{k}}$. Since $\gamma_{\mathbf{k}_{AFM}}=0$ the relevant (pseudo)gap scale is

$$\Delta^{PG}_{\mathbf{k}}=|\Delta_{\mathbf{k}_{AFM}}|=\frac{Z^{\rm ef}_{\mathbf{k}}}{2}\sqrt{r_s}|2J-4t'\cos^2 k_x|. \tag{37}$$

It is instructive to realize that $\Delta^{PG}_{\mathbf{k}}$ does not depend on t, but rather on smaller J and in particular t'. For $t'<0$ the gap is largest at $(\pi,0)$, consistent with experiments. The (pseudo)gap that appears at the Fermi energy $\omega=0$ depends, however, on properties of $\epsilon^{\rm ef}_{\mathbf{k}_{AFM}}$. We do not expect that the gap opens along the whole AFM zone boundary, since in most cases $\epsilon^{\rm ef}_{\mathbf{k}_{AFM}}$ crosses zero along $(\pi/2,\pi/2)$-$(\pi,0)$ so that within the QSA $E^-_{\mathbf{k}}$ forms a hole-pocket-like FS. In fact, the results of the QSA are equivalent to the system with long-range spin-density-wave order (an AFM), where the doubling of the unit cell appears.

Within the simplified effective band approach [Eq. (31)], it is not difficult to evaluate numerically $\Sigma_{\rm lf}$ also beyond the QSA, by explicitly taking $\chi(\mathbf{q},\omega)$ [Eq. (29)], for $\kappa>0$ and $\omega_\kappa=2J\kappa$. Integrals in Eq. (24) can be performed mostly analytically if we linearize the dependence of $\epsilon^{\rm ef}_{\mathbf{k}}$ within the relevant interval $\delta k\lesssim\kappa$.

Let us, for illustration, present in this section results characteristic for the development of spectral functions with the most sensitive parameters κ and μ, which both simulate the variation with doping. We further fix on the model parameter $J/t=0.3$ as relevant for cuprates. Here we take $t'/t=-0.3$, close to values quoted for BSCCO. For simplicity we assume first that the effective band $\epsilon^{\rm ef}_{\mathbf{k}}$ is just renormalized $\epsilon_{\mathbf{k}}$ (justified for an intermediate doping; see Sec. V) with fixed values $t_{\rm ef}/t=0.3$, $t'_{\rm ef}/t=-0.1$, and $Z^{\rm ef}=0.4$. A more realistic treatment would require the variation of latter parameters with c_h, but the results remain qualitatively similar. We take $\kappa\sim\sqrt{c_h}$ in accord with experiments[1] and numerical results on the t-J model.[33,9,32]

The choice of μ is somewhat more arbitrary since, within an effective-band approach the sum rule [Eq. (30)], cannot be used as a criterion. Nevertheless it is evident that μ determines the shape and volume of the FS. In the following examples we choose μ such that at given κ the DOS at the Fermi energy, $\mathcal{N}(0)$, reaches a local minimum. This means that effectively the states near the $(\pi,0)$ are in the pseudogap and that the truncation of the FS is most pronounced (at given κ). Such a choice of μ in fact also yields the volume of the FS (except at extreme $\kappa\ll 1$) quite close to the one consistent with the Luttinger theorem.[34]

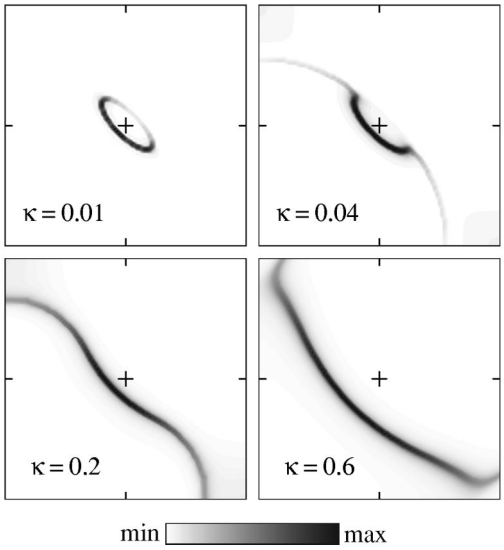

FIG. 1. Contour plot of spectral functions $A(\mathbf{k},\omega=0)$ at $T=0$ for various κ in one quarter of the Brillouin zone.

In Fig. 1 we first present results for $A(\mathbf{k},\omega=0)$ at $T=0$ for a broad range of $\kappa=0.01$–0.6. Curves (evaluated at small additional smearing $\epsilon=0.02t$) in fact display the effective FS determined by the condition $G^{-1}(\mathbf{k}_F,0)=0$. At the same time, intensities $A(\mathbf{k},\omega=0)$ correspond to the renormalization factor Z_F. We can comment upon the development as follows. At extremely small $\kappa=0.01$ we see the hole-pocket FS which follows from the QSA in Eq. (36). In spite of the small κ the ''shadow'' side of the hole pocket has a smaller Z_F. Already the small $\kappa\sim 0.05$ destroys the shadow side of the pocket, i.e., the solution $G^{-1}=0$ on the latter side disappears since the singularity in $\Sigma_{\rm lf}$ [Eq. (35)], is smeared out by finite κ. On the other hand, in the gap emerge QP solutions with very weak $Z_F\ll 1$ which reconnect the FS into a large one. We are dealing nevertheless with an effectively truncated FS with well-developed arcs. The effect of larger κ is essentially to increase Z_F in the gapped region, in particular near $(\pi,0)$. Finally, for large $\kappa=0.6$, which corresponds to the regime consistent with optimal doping or overdoping in cuprates, Z_F is essentially only weakly decreasing toward $(\pi,0)$, and the FS is well pronounced and concave as naturally expected for $t'<0$.

In order to understand the pseudogap features at low but finite κ, in Figs. 2 and 3 we present $A(\mathbf{k},\omega)$ for $\kappa=0.1$. The spectra in Fig. 3 are presented along the lines a–c in the Brillouin zone as shown in Fig. 2. As expected from Eq. (36), the pseudogap is smallest along the zone diagonal (line a) where, moreover, the pseudogap appears at $\omega>0$, so that it would not be seen in ARPES. Lines a and b are thus examples of the region where arcs of the FS are well pronounced, i.e., their QP weight is not strongly renormalized: $Z_F\lesssim Z^{\rm ef}$. On the other hand, following line c the chemical potential $\omega=0$ falls into the pseudogap. We see in Fig. 3(a) that QP in fact crosses coherently the FS ($\omega=0$) although

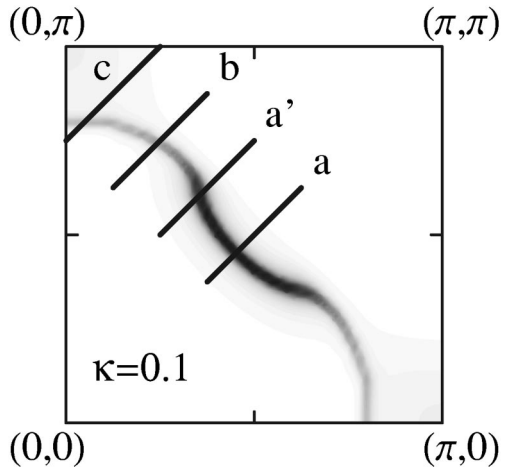

FIG. 2. $A(\mathbf{k},\omega=0)$ for $\kappa=0.1$ and lines (a)–(c) used in Fig. 3.

with very small $Z_F \ll 1$. It is evident from Fig. 1 that Z_F within the pseudogap remains small only for $\kappa \ll 1$ while it increases and finally smears out the concept of the pseudogap for $\kappa \gtrsim \kappa^* \sim 0.5$.

It is quite remarkable to note that in spite of $Z_F \ll 1$ the QP velocity v_F is not diminished within the pseudogap. In fact it is even enhanced, as seen in Fig. 3(b), and the QP is well defined at the FS, while it becomes fuzzy at $\omega \neq 0$ merging with the solutions $E_{\mathbf{k}}^{\pm}$, respectively, away from the FS.

The presented formalism offers a possible scenario for the evolution of the FS with doping from a pocketlike surface into a large surface. In order to explain results in Fig. 3 concerning the effective truncation of the FS and the character of the QP within the pseudogap, we note that it is essentially enough that both κ and ω_κ are finite to yield a well-defined FS. Since gross features do not depend on the particular form of Eq. (29), here we present a simplified analysis using

$$\chi'(\mathbf{Q}+\tilde{\mathbf{q}},\omega)=\begin{cases} C[\,\delta(\omega-\omega_\kappa)-\delta(\omega+\omega_\kappa)], & \tilde{q}_\perp<\kappa \\ 0, & \tilde{q}_\perp>\kappa, \end{cases} \tag{38}$$

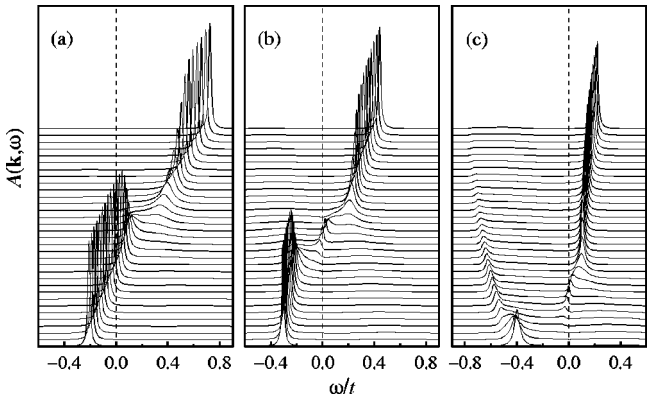

FIG. 3. $A(\mathbf{k},\omega)$ for $\kappa=0.1$ along different directions (a), (b), and (c) in the Brillouin zone, corresponding to Fig. 2. Spectra for (a′) from Fig. 2 are very similar to (a).

where $\tilde{q}_\perp$ denotes the component perpendicular to the antiferromagnetic zone boundary. Let us assume that $\epsilon_{\mathbf{k}}^{\mathrm{ef}}-\mu=\epsilon\sim 0$ and $\epsilon_{\mathbf{k}-\mathbf{Q}}^{\mathrm{ef}}-\mu=\bar{\epsilon}\sim 0$. We also linearize dispersion $\epsilon_{\mathbf{k}}^{\mathrm{ef}}$ at the FS, and assume that $\mathbf{v}_{\mathbf{k}}^{\mathrm{ef}}\|(1,1)$, so that from Eq. (25) we obtain

$$\Sigma(\epsilon,\omega)=-\frac{\Delta^2}{2w}\log\frac{(w+\omega_\kappa+\bar{\epsilon}-\omega)(\omega_\kappa+\omega)}{(w+\omega_\kappa-\bar{\epsilon}+\omega)(\omega_\kappa-\omega)}, \tag{39}$$

where $w=v_{\mathbf{k}}^{\mathrm{ef}}\kappa$ and $\Delta=\Delta_{\mathbf{k}}$. Let us evaluate QP properties on the FS assuming that it is located at $\bar{\epsilon}=0$, i.e., on the antiferromagnetic zone boundary. From Eq. (39) we obtain the QP weight Z_F

$$\frac{Z_F}{Z^{\mathrm{ef}}}=\left[1-\frac{\partial\Sigma'}{\partial\omega}\bigg|_{\omega=0,\bar{\epsilon}=0}\right]^{-1}=\left[1+\frac{\Delta^2}{\omega_\kappa(\omega_\kappa+w)}\right]^{-1}. \tag{40}$$

This clearly leads to $Z_F \ll 1$ for $\omega_\kappa w \sim 2v_{\mathbf{k}}^{\mathrm{ef}} J\kappa^2 \ll \Delta^2$. This is generally the case within the gapped part of the FS for small $\kappa<\kappa^*$, as shown in Fig. 1. It should be also noted that the latter condition is essentially always satisfied near $(\pi,0)$ where $v_{\mathbf{k}}^{\mathrm{ef}}\sim 0$ and consequently also $w\sim 0$.

Let us evaluate in the same way the QP renormalized velocity $v(\mathbf{k}_F)$ at the FS. Here we realize that the $\mathbf{k}$ dependence of Σ' is essential. The latter is given in Eq. (40) by the ϵ dependence,

$$\frac{v(\mathbf{k}_F)}{v_{\mathbf{k}}^{\mathrm{ef}}}=\left(1+\frac{\partial\Sigma'}{\partial\epsilon}\right)\frac{Z_F}{Z^{\mathrm{ef}}},$$

$$\frac{\partial\Sigma'}{\partial\epsilon}\Big|_{\omega=0,\bar{\epsilon}=0}=\frac{\Delta^2}{\omega_\kappa(\omega_\kappa+w)}, \tag{41}$$

which, in contrast to Z_F, leads to an enhancement of v_F. In the case $\omega_\kappa w \ll \Delta^2$ we thus obtain

$$\frac{v_F}{v_{\mathbf{k}}^{\mathrm{ef}}}\sim\frac{\omega_\kappa}{w}\sim\frac{2J}{v_{\mathbf{k}}}. \tag{42}$$

The final $v(\mathbf{k}_F)$ is therefore not strongly renormalized, since $2J$ and $v_{\mathbf{k}}^{\mathrm{ef}}$ are of similar order. Furthermore, $v(\mathbf{k}_F)$ is enhanced in the parts of the FS where $v_{\mathbf{k}}^{\mathrm{ef}}$ is small, in particular near the $(\pi,0)$ point. The situation is thus very different from ''local'' theories where $\Sigma(\mathbf{k},\omega)\sim\Sigma(\omega)$ and the QP renormalization is governed only by Z_F. In our case the ''nonlocal'' character of $\Sigma(\mathbf{k},\omega)$ is essential in order to properly describe the QP within the pseudogap region.

Let us further discuss the behavior of the DOS $\mathcal{N}(\omega)$ [Eq. (30)]. It is evident from Fig. 1 that the contribution to $\mathcal{N}(\omega\sim 0)$ will come mostly from FS arcs near the zone diagonal, while the gapped regions near $(\pi,0)$ will contribute less. Results presented in Fig. 4 (full lines) show the development of $\mathcal{N}(\omega)$ with κ, as corresponding to the FS in Fig. 1. We see that the DOS indeed reveals a pseudogap at $\omega<\Delta$; however, the pseudogap is visible only for $\kappa<0.5$ and deepens for $\kappa\rightarrow 0$.

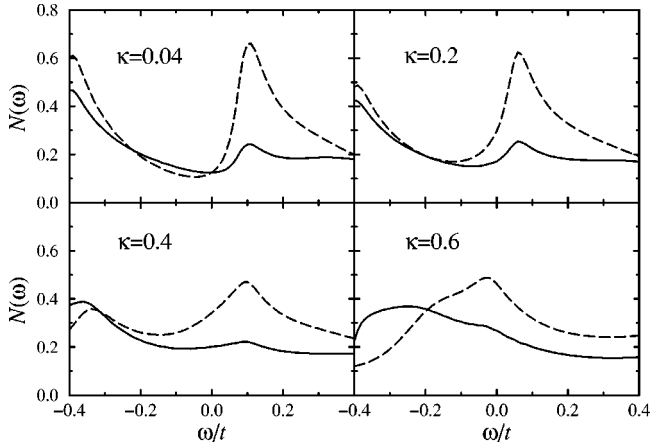

FIG. 4. Density of states $\mathcal{N}(\omega)$ (full lines) and weighted DOS $\mathcal{N}_w(\omega)$ (dashed lines) for different κ.

The DOS is measured in cuprates via angle-integrated PES, e.g., for LSCO in Ref. 35, as well as via scanning tunneling microscopy (STM).[36] It is very possible that within both experiments the matrix elements are essentially leading to enhanced contribution near the x points in the Brillouin zone. It has been proposed that for the c-axis conductivity[37] the interplanar hopping should be weighted by the matrix element

$$w(\mathbf{k}) = (\cos k_x - \cos k_y)^2. \tag{43}$$

The same arguments as for the c-axis conductivity might apply also for the STM effective DOS as well as for integrated PES, therefore, we also present the weighted DOS $\mathcal{N}_w$ where $w(\mathbf{k})$ is introduced additionally into Eq. (30). Results also presented in Fig. 4 (dashed line) show a much more strongly pronounced pseudogap, in particular at low κ. This is quite evident since $w(\mathbf{k})$ essentially destroys the effect of FS arcs near $(\pi/2,\pi/2)$, which present the main contribution (due to small velocity in hole-pocket FS) to the usual $\mathcal{N}(\omega)$.

In Fig. 5(a) we show the average $Z_{\rm av}$ along the FS, as well as the QP DOS, defined as

$$\mathcal{N}_{QP} = \frac{1}{2\pi^2} \oint \frac{dS_F}{v(\mathbf{k}_F)}. \tag{44}$$

In Fig. 5(b) we present, as well as the dependence of the DOS at the FS, both $\mathcal{N}(0)$ and $\mathcal{N}_w(0)$ as functions of κ. Note that $\mathcal{N}_{QP}$ should be relevant for the specific heat, i.e., $\mathcal{N}_{QP} \propto \gamma = C_V/T$ at low T (provided that we are dealing with a normal Fermi liquid). It is quite important to understand that decreasing κ (smaller doping) also means decreasing $\mathcal{N}_{QP}$, which is also consistent with the observation of a pseudogap in the specific heat in cuprates.[38] Here we note that such a behavior is not evident when one discusses the metal-insulator transition. That is, in a Fermi liquid with a (nearly) constant Fermi surface one can drive the metal-insulator transition by $Z_{\rm av} \to 0$, and within the assumption of a local character $\Sigma(\omega)$ this would lead to $v_F \to 0$ and consequently to $\mathcal{N}_{QP} \to \infty$. Clearly, the essential difference in our case is that within the pseudogap regime $\Sigma(\mathbf{k},\omega)$ is nonlocal, allowing for the simultaneous decrease of $\mathcal{N}(0)$ and $\mathcal{N}_{QP}$.

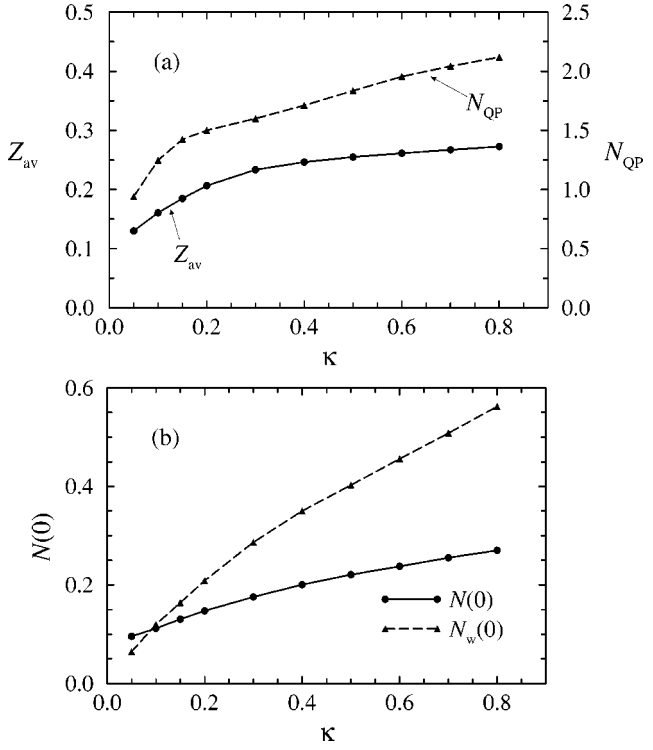

FIG. 5. (a) Average QP weight $Z_{\rm av}$ and QP DOS $\mathcal{N}_{\rm QP}$ vs κ. (b) DOS $\mathcal{N}(0)$ and weighted DOS $\mathcal{N}_{\rm w}(0)$ vs κ.

Finally, let us comment on the influence of finite T. While T also enters within this approach via effective parameters as $v_{\mathbf{k}}^{\rm ef}$ and predominantly $\kappa(T)$, here we consider only the direct effect via the thermodynamic factor in Eq. (25). It is evident that $T>0$ smears out $\Sigma_{\rm lf}$. This becomes important at small κ in particular for QP's in the pseudogap regime. In Fig. 6 we present $A(\mathbf{k},\omega)$, corresponding to Fig. 3(b), for several values of low T. The main conclusion is that a weak (but sharp) QP peak with $Z_F \ll 1$ at $T=0$ is smeared out already by very

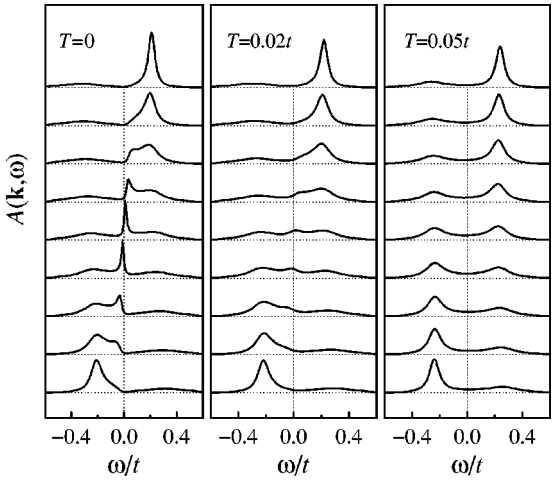

FIG. 6. $A(\mathbf{k},\omega)$ for $\kappa=0.1$ and $\mathbf{k}$ along the central part of the line b in Fig. 2 for various T: $T=0$, $T=0.02t$, and $T=0.05t$. The momentum $\mathbf{k}$ ranges from $(\pi/4,3\pi/4) \mp (\pi/32,\pi/32)$.

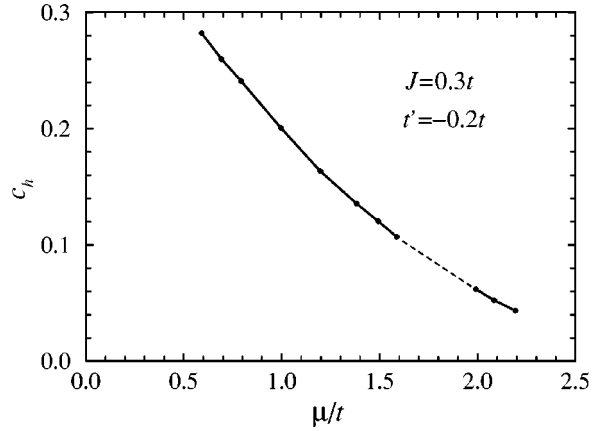

FIG. 7. Hole doping c_h as a function of the chemical potential μ/t, following from the self-consistent calculation.

small $T>T^s\sim 0.02\ t$ and is not at all visible (there is no overdamped peak) at higher T, the remainder being an incoherent background at $\omega\sim 0$ for $T>T^s$. This is important to realize that ARPES experiments in fact do not observe a well-defined QP peak near $(\pi,0)$ in the underdoped regime at $T>T_c$.

V. SELF-CONSISTENT CALCULATION

The full self-consistent sets of equations for $\Sigma=\Sigma_{\rm pm}+\Sigma_{\rm lf}$ [Eqs. (22) and (24)], and for G [Eq. (15)], are solved numerically. For given μ the FS emerges as a solution determined by the relation $\zeta_{\mathbf{k}_F}+\Sigma'(\mathbf{k}_F,0)=\mu$. We should note that, at a given μ, the electron concentration c_e as calculated from the DOS $\mathcal{N}(\omega)$ [Eq. (31)], does not in general coincide with the one evaluated from the FS volume, $\tilde{c}_e=V_{\rm FS}/V_0$. Nevertheless, apart from the fact that within the t-J model the validity of the Luttinger theorem is under question,[39] in regimes of large FS's both quantities appear to be quite close. Within the presented theory the position of the FS is mainly determined by $\zeta_{\mathbf{k}}$ and $\Sigma_{\rm pm}$ and is less sensitive to $\Sigma_{\rm lf}$. On the other hand, $\Sigma_{\rm lf}$ is crucial for the QP properties near the FS.

As discussed in Sec. III, in Eq. (7) we use the most appropriate and simplest approximation to insert the unrenormalized $A^0(\mathbf{k},\omega)$, i.e., the spectral function without a self-consistent consideration of $\Sigma_{\rm lf}$ but with $\Sigma_{\rm pm}$ fully taken into account. Here we choose $t'=-0.2t$ and again $\kappa=\sqrt{c_h}$, while η_1 and η_2 are determined as a function of c_h from model calculations.[33] We use $N=40\times 40$ points in the Brillouin zone and broadening $\epsilon/t=0.05$.

In Fig. 7 we present hole concentration c_h vs μ as obtained from $\mathcal{N}(\omega)$ at $T=0$. We solve self-consistent equations by iteration, whereby for $0.06<c_h<0.11$ we find in the equations an instability signaled by oscillatory behavior instead of the convergence; a unique solution cannot be obtained in the region indicated by the dashed line. However, at lower (and higher) doping the solution is converged. It seems that the region of instability coincides with the transition from the large to a small FS.

The shape of the FS is most clearly presented with contour plot of the electron momentum distribution function defined as

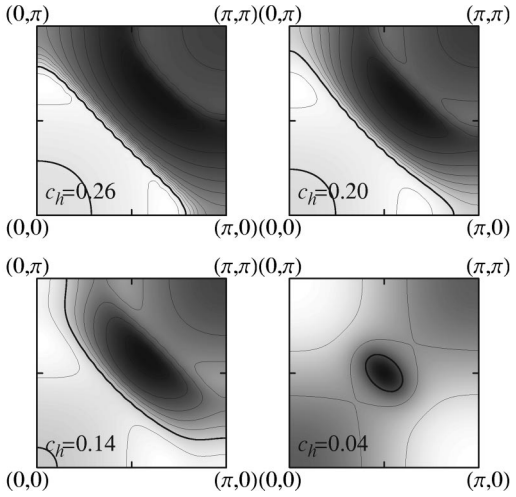

FIG. 8. Electron momentum distribution $\tilde{n}(\mathbf{k})$ for various c_h. Thin contour lines represent $\tilde{n}(\mathbf{k})$ in increments of 0.05, while the heavy line corresponds to $\tilde{n}(\mathbf{k})=0.8$ for $c_h=0.26$, 0.20, 0.14, and $\tilde{n}(\mathbf{k})=0.85$ for $c_h=0.04$.

$$\tilde{n}(\mathbf{k})=\alpha^{-1}\int_{-\infty}^{0}A(\mathbf{k},\omega)\,d\omega. \tag{45}$$

Results for a characteristic development of the FS with c_h are shown in Fig. 8. At higher doping, $c_h=0.26$ and also $c_h=0.20$, we obtain a common large FS topology. In the intermediate doping regime, $c_h=0.14$, the pseudogap is pronounced at momenta around $(\pi,0)$ and the FS shows a tendency to form a small FS. The gap is more pronounced because of longer antiferromagnetic correlation length ξ (smaller κ). At $c_h<c_h^0\sim 0.06$ solutions are consistent with a small pocketlike FS, whereby this behavior is enhanced by $t'<0$, as realized in other model studies.[10] On increasing doping the FS rather abruptly changes from small to large, as suggested from the results of the SCBA.[40] The smallness of c_h^0 has the origin in the quite weak dispersion dominated by J and t' at $c_h\to 0$ which is overshadowed by much larger $\zeta_{\mathbf{k}}$ at moderate doping, where the FS is large and its shape is controlled by t'/t.

In Figs. 9(a) and 9(b) we present calculated $A(\mathbf{k},\omega)$ along the principal directions in the Brillouin zone, i.e., $(\pi/2,\pi/2)\to(0,0)\to(\pi,0)$. It is evident that $\Sigma_{\rm pm}$ leads to a strong damping of hole QP and a quite incoherent momentum-independent spectrum $A(\mathbf{k},\omega)$ for $\omega\ll -J$ which qualitatively reproduces ARPES and numerical results.[13] Electron QP's (at $\omega>0$) are in general very different, i.e., with much weaker damping arising only from $\Sigma_{\rm pm}$. Note the relatively high QP velocity in the higher doping regime $c_h=0.26$ [Fig. 9(a)], as compared to a more narrow dispersion on the scale $2J$ at low doping $c_h=0.04$ [Fig. 9(b)], where we find a regime of small pocketlike FS's.

In Fig. 10 we present the development of spectral functions at fixed $c_h=0.2$, but now varying κ as an independent

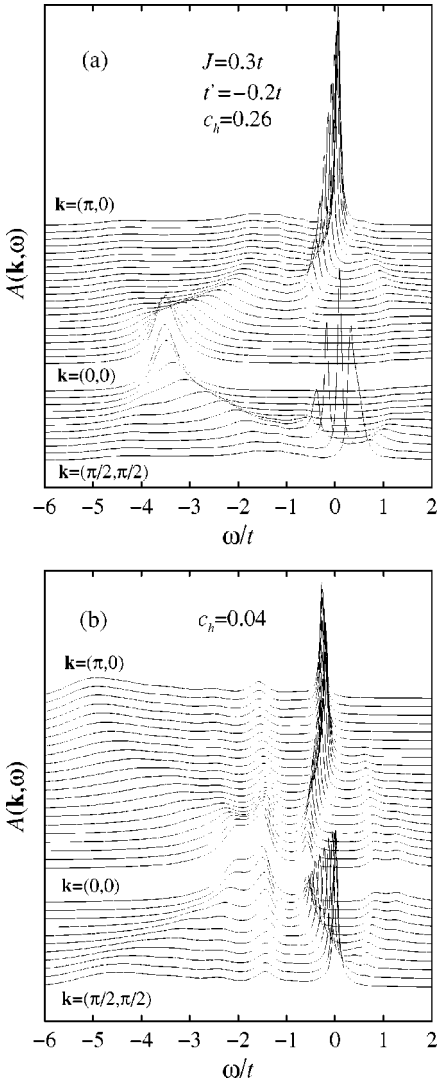

FIG. 9. $A(\mathbf{k},\omega)$ along main directions in the Brillouin zone.

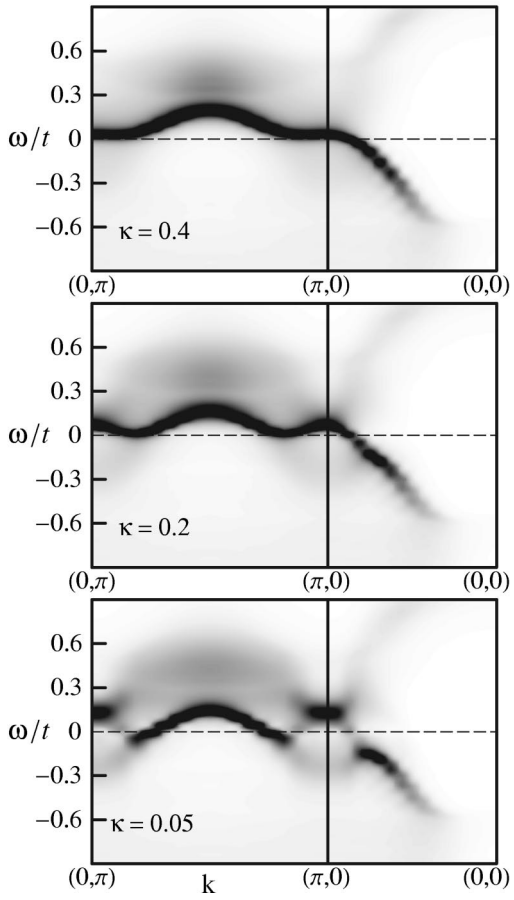

FIG. 10. Contour plot of $A(\mathbf{k},\omega)$ for fixed doping $c_h=0.2$ and various κ.

parameter. Let us concentrate on the emergence of the pseudogap near $(\pi,0)$. At $\kappa=0.4\sim\sqrt{c_h}$ the pseudogap is essentially not yet developed. Nevertheless, the gap opens with decreasing κ, in particular for (at this doping unrealistic value) $\kappa=0.05$.

VI. CONCLUSIONS

We have presented the theory of spectral functions within the t-J model, whereby our method is based on EQM for projected fermionic operators and on the decoupling approximation for the self-energy, assuming the fermions and spin fluctuations as essential coupled degrees of freedom. We first make some comments on the method.

(a) The EQM approach for spectral functions (as well as for other dynamical quantities) seems to be promising, since it can exactly treat the constraint which is essential for the physics of strongly correlated electrons.

(b) In finding the proper approximation for the self-energy within the EQM approach it is plausible that the main ingredient is the coupling of fermions with spin fluctuations, where close to the antiferromagnetically ordered state both short-range transverse and longer-range (longitudinal) spin fluctuations are important. It is very possible, however, that other contributions could be important, e.g., the coupling to pairing fluctuations.

(c) In an ordered AFM our method naturally reproduces the results for the spectral function (of a hole) within the SCBA, which is highly nontrivial, since both approaches are quite different.

(d) The coupling to longitudinal spin fluctuations appears to be most important for QP's near the AFM zone boundary, and is responsible for the opening of the pseudogap. Here the coupling is only moderately strong, and can be treated in the lowest-order decoupling scheme.

(e) The present theory uses the spin response as an input. $\chi''(\mathbf{q},\omega)$ [Eq. (29)] corresponds in general to a Fermi liquid or to a short-range AFM liquid. Results remain, in fact, qualitatively similar as far as $\chi''(\mathbf{q},\omega)$ is nonsingular. In the opposite case, e.g., if we would use the marginal Fermi liquid (MFL) form as an input, the Fermi surface would still be defined, but the QP would have a vanishing weight $Z\to 0$.[23]

Let us further discuss some main results of the presented theory:

(a) The fermion-paramagnon coupling as manifested in $\Sigma_{\rm pm}$ remains effective and strong even at moderate doping. The full calculation shows that the coupling leads to a large

incoherent part in the hole part ($\omega<0$) of the spectral function, as well as to the renormalized band $\epsilon_{\mathbf{k}}^{\mathrm{ef}}$.

(b) The main consequence of Σ_{lf} due to the coupling to longer-range longitudinal spin fluctuations is the appearance of a pseudogap at $\kappa<\kappa^*$. The pseudogap opens predominantly along the AFM zone boundary, and its extent is qualitatively given by Eq. (37), dependent on J and t' but not directly on t. Evidently the pseudogap has a similarity to the d-wave-like dependence along the FS, for $t'<0$ being largest near the $(\pi,0)$ point.

(c) How strong the pseudogap effect is depends mainly on κ. At small $\kappa\ll\kappa^*$ parts of the Fermi surface near $(\pi/2,\pi/2)$ remain well pronounced (for $t'<0$) while the Fermi surface within the pseudogap is suppressed, i.e., QP's have a small weight $Z_F\ll 1$, in particular near zone corners $(\pi,0)$.

(d) The simplified analysis yields large Fermi surface, although a truncated one, except at very small $\kappa\ll\kappa^*$ where Σ_{lf} by itself induces a small hole-pocket-like Fermi surface. On the other hand, Σ_{pm} generates hole pockets already for $c_h<c_h^0\sim 0.06$. In fact, an instability of the self-consistent calculation indicates the emergence of a hole-pocket Fermi surface even at $c_h\lesssim 0.1$. However, it is very possible that within the present approximation scheme Σ_{pm} is overestimated at intermediate c_h, an indication for it being quite a weak dispersion $\epsilon_{\mathbf{k}}^{\mathrm{ef}}$.

(e) Our method is approximate in the evaluation of Σ, hence it is not surprising that the volume of the Fermi surface does in general not coincide with the one following from the Luttinger theorem. In any case it is questionable if such a relation should be valid within the t-J model[39] due to the projected basis and strong correlations. Nevertheless, in the regime of a large Fermi-surface the full calculation yields the Fermi surface volume quite close to the Luttinger one.

(f) For $\kappa<\kappa^*$ the QP within the pseudogap has a small weight $Z_F\ll 1$ but not a diminished $v(\mathbf{k}_F)$, which is the effect of the nonlocal character of $\Sigma(\mathbf{k},\omega)$. A consequence is that QP's within the pseudogap contribute much less to the QP DOS $\mathcal{N}_{QP}$. This can explain the reduction of the latter with doping and the appearance of the pseudogap in the specific heat being essential for the understanding of the specific heat in underdoped cuprates.

(g) Although most results are presented for $T=0$, we can discuss some effects of $T>0$. The first effect is that within the pseudogap the QP's with $Z_F\ll 1$ are already washed out (not just overdamped) for very small $T<T^s\ll\Delta^{PG}$. On the other hand, the pseudogap is mainly affected by κ. So we can argue that the pseudogap would be observable for $\kappa(c_h,T)<\kappa^*\sim 0.5$. This effectively determines the pseudogap crossover temperature $T^*(c_h)$. From the quantitative studies of the t-J model,[41,32] it appears that in the region of interest κ is nearly linear in both T and c_h so we would approximately obtain

$$T^*\sim T_0^*(1-c_h/c_h^*), \tag{46}$$

where $T_0^*\sim 0.6J$ and $c_h^*\sim 0.15$.

Finally we make some comments on the relevance of our results to experiments on cuprates, in particular with respect to observed pseudogap and Fermi surface features.

(a) The (large) pseudogap scale shows up, in ARPES on BSCCO, as a hump at ~ 100 eV.[2] Our results indicate quite a similar pseudogap scale, e.g., in the DOS in Fig. 4 the $\omega<0$ pseudogap $\sim 0.3\ t$ (note that $t\sim 0.4$ eV), since Δ^{PG} is determined mainly by J and t'. The pseudogap and the hump are also very visible in spectral functions $A(\mathbf{k},\omega)$ with $\mathbf{k}\sim(\pi,0)$, e.g., in Fig. 6(a). However, it should be noted that $\kappa=0.1$ in Figs. 3 and 6 is already quite small, and leads to QP peaks being too narrow relative to experiments.

(b) The truncated Fermi surface in underdoped BSCCO appears as an arc (part of the large Fermi surface corresponding to $t'<0$) in the Brillouin zone,[3] effectively not crossing the antiferromagnetic zone boundary, which is also characteristic of our results for $\kappa<\kappa^*$, originating from the strong coupling to spin fluctuations with commensurate (π,π). The same is true of the origin of shadow features in spectral functions pronounced at intermediate doping and in particular at weak doping.

(c) Our results for the depletion of the DOS $\mathcal{N}(0)$ $[\mathcal{N}_w(0)]$ with decreasing doping are qualitatively consistent with the integrated PES [so far known for LSCO (Ref. 35)] and STM,[36] although in this relation the importance of matrix element corrections is not yet clarified. In relation to STM results[36] we note that our DOS's are not as symmetric around $\omega=0$. In general, however, the DOS's at low doping cannot be very symmetric since the DOS sum rule is essentially different for the electron $\omega>0$ part $\propto 2c_h$ and the hole $\omega<0$ part $\propto 1-c_h$.

(d) We also find a decrease of the QP DOS $\mathcal{N}_{QP}$ with doping, essential in connection with the specific-heat pseudogap in underdoped cuprates.[38] However, it should be mentioned that our results for both $\mathcal{N}(0)$ as well as $\mathcal{N}_{QP}$ $\propto\gamma$ indicate a weaker suppression with decreasing doping than observed in experiments. This is due to remaining contribution of Fermi-surface arcs, which could be overestimated in our approach for $\kappa\ll\kappa^*$.

(e) Both the value and dependence of the pseudogap temperature $T^*(c_h)$, as estimated in Eq. (46), seem to be very reasonable in connection with experimental evidence, arising from various transport and magnetic properties in cuprates.[1]

[1] For a review see, e.g., M. Imada, A. Fujimori, and Y. Tokura, Rev. Mod. Phys. **70**, 1039 (1998).

[2] D.S. Marshall *et al.*, Phys. Rev. Lett. **76**, 4841 (1996); H. Ding *et al.*, Nature (London) **382**, 51 (1996).

[3] M.R. Norman *et al.*, Nature (London) **392**, 157 (1998).

[4] A. Fujimori *et al.*, in *Open Problems in Strongly Correlated Electron Systems*, Vol. 15 of NATO Science Series, edited by J. Bonča, P. Prelovšek, A. Ramšak, and S. Sarkar (Kluwer, Dordrecht, 2001).

[5] C.L. Kane, P.A. Lee, and N. Read, Phys. Rev. B **39**, 6880 (1989).

[6] A. Ramšak and P. Prelovšek, Phys. Rev. B **42**, 10 415 (1990); G. Martínez and P. Horsch, *ibid.* **44**, 317 (1991).
[7] B.O. Wells *et al.*, Phys. Rev. Lett. **74**, 964 (1995).
[8] F. Ronning *et al.*, Science **282**, 2067 (1998).
[9] For a review, see E. Dagotto, Rev. Mod. Phys. **66**, 763 (1994).
[10] T. Tohyama and S. Maekawa, J. Phys. Soc. Jpn. **59**, 1760 (1990); Supercond. Sci. Technol. **13**, R17 (2000).
[11] W. Stephan and P. Horsch, Phys. Rev. Lett. **66**, 2258 (1991).
[12] J. Jaklič and P. Prelovšek, Phys. Rev. B **55**, R7307 (1997); P. Prelovšek, J. Jaklič, and K. Bedell, *ibid.* **60**, 40 (1999).
[13] For a review, see J. Jaklič and P. Prelovšek, Adv. Phys. **49**, 1 (2000).
[14] C.M. Varma, P.B. Littlewood, S. Schmitt-Rink, E. Abrahams, and A.E. Ruckenstein, Phys. Rev. Lett. **63**, 1996 (1989).
[15] R. Preuss, W. Hanke, C. Gröber, and H.G. Evertz, Phys. Rev. Lett. **79**, 1122 (1997).
[16] A. Kampf and J.R. Schrieffer, Phys. Rev. B **41**, 6399 (1990).
[17] N.E. Bickers, D.J. Scalapino, and S.R. White, Phys. Rev. Lett. **62**, 961 (1989); M. Langer, J. Schmalian, S. Grabowski, and K.H. Bennemann, *ibid.* **75**, 4508 (1995).
[18] Z. Wang, Y. Bang, and G. Kotliar, Phys. Rev. Lett. **67**, 2733 (1991).
[19] P. Monthoux, A.V. Balatsky, and D. Pines, Phys. Rev. Lett. **67**, 3448 (1991); Phys. Rev. B **46**, 14 803 (1992); P. Monthoux and D. Pines, *ibid.* **47**, 6069 (1993).
[20] A.V. Chubukov and D.K. Morr, Phys. Rep. **288**, 355 (1997).
[21] J. Schmalian, D. Pines, and B. Stojković, Phys. Rev. Lett. **80**, 3839 (1998); Phys. Rev. B **60**, 667 (1999).
[22] D. Zanchi and H.J. Schulz, Europhys. Lett. **44**, 235 (1997); N. Furukawa, T.M. Rice, and M. Salmhofer, Phys. Rev. Lett. **81**, 3195 (1998).
[23] P. Prelovšek, Z. Phys. B: Condens. Matter **103**, 363 (1997).
[24] N.M. Plakida and V.S. Oudovenko, Phys. Rev. B **59**, 11 949 (1999).
[25] S. Onoda and M. Imada, J. Phys. Soc. Jpn. **70**, 632 (2001).
[26] P. Prelovšek and A. Ramšak, Phys. Rev. B **63**, 180506 (2001).
[27] D.N. Zubarev, Usp. Fiz. Nauk. **71**, 71 (1960) [Sov. Phys. Usp. **3**, 320 (1960)].
[28] H. Mori, Prog. Theor. Phys. **33**, 423 (1965).
[29] W. Götze and P. Wölfle, Phys. Rev. B **6**, 1226 (1972).
[30] P.A. Lee, T.M. Rice, and P.W. Anderson, Phys. Rev. Lett. **31**, 462 (1973).
[31] A.J. Millis and H. Monien, Phys. Rev. B **61**, 12 496 (2000).
[32] R.R.P. Singh and R.L. Glenister, Phys. Rev. B **46**, 11 871 (1992).
[33] J. Bonča, P. Prelovšek, and I. Sega, Europhys. Lett. **10**, 87 (1989).
[34] J.M. Luttinger, Phys. Rev. **119**, 1153 (1960).
[35] A. Ino *et al.*, Phys. Rev. Lett. **81**, 2124 (1998).
[36] Ch. Renner, B. Revaz, K. Kadowaki, I. Maggio-Aprile, and O. Fischer, Phys. Rev. Lett. **80**, 3606 (1998).
[37] L.B. Ioffe and A.J. Millis, Phys. Rev. B **58**, 11 631 (1998).
[38] J.W. Loram, K.A. Mirza, J.R. Cooper, and W.Y. Liang, Phys. Rev. Lett. **71**, 1740 (1993); J.W. Loram, J.L. Luo, J.R. Cooper, W.Y. Liang, and J.L. Tallon, Physica C **341-8**, 831 (2000).
[39] W.O. Putikka, M.U. Luchini, and R.R.P. Singh, Phys. Rev. Lett. **81**, 2966 (1998).
[40] A. Ramšak, I. Sega, and P. Prelovšek, Phys. Rev. B **61**, 4389 (2000).
[41] A. Sokol, R.L. Glenister, and R.R.P. Singh, Phys. Rev. Lett. **72**, 1549 (1994).